Stochastic Dynamic Causal Modelling of fMRI Data with Multiple-Model Kalman Filters

P. Osório[1,2]; P. Rosa[1,3,4]; C. Silvestre[5]; P. Figueiredo[1,2]

[1]Institute for Systems and Robotics, Lisbon, Portugal;
[2]Department of Bioengineering, Instituto Superior Técnico, Universidade de Lisboa, Lisbon, Portugal;
[3]Department of Electrical and Computer Engineering, Instituto Superior Técnico, Universidade de Lisboa, Lisbon, Portugal;
[4]Deimos Engenharia, Lisbon, Portugal;
[5]Department of Electrical and Computer Engineering, Faculty of Science and Technology, University of Macau, Macau, China

Keywords

Stochastic, DCM, fMRI, Multiple-Model Kalman Filter

Summary

Introduction: This article is part of the Focus Theme of Methods of Information in Medicine on "Biosignal Interpretation: Advanced Methods for Neural Signals and Images".

Background: Dynamic Causal Modelling (DCM) is a generic formalism to study effective brain connectivity based on neuroimaging data, particularly functional Magnetic Resonance Imaging (fMRI). Recently, there have been attempts at modifying this model to allow for stochastic disturbances in the states of the model.

Objectives: This paper proposes the Multiple-Model Kalman Filtering (MMKF) technique as a stochastic identification model discriminating among different hypothetical connectivity structures in the DCM framework; moreover, the performance compared to a similar deterministic identification model is assessed.

Methods: The integration of the stochastic DCM equations is first presented, and a MMKF algorithm is then developed to perform model selection based on these equations. Monte Carlo simulations are performed in order to investigate the ability of MMKF to distinguish between different connectivity structures and to estimate hidden states under both deterministic and stochastic DCM.

Results: The simulations show that the proposed MMKF algorithm was able to successfully select the correct connectivity model structure from a set of pre-specified plausible alternatives. Moreover, the stochastic approach by MMKF was more effective compared to its deterministic counterpart, both in the selection of the correct connectivity structure and in the estimation of the hidden states.

Conclusions: These results demonstrate the applicability of a MMKF approach to the study of effective brain connectivity using DCM, particularly when a stochastic formulation is desirable.

Correspondence to:
Patrícia Figueiredo, D. Phil.
Institute for Systems and Robotics
Department of Bioengineering
Instituto Superior Técnico
Universidade de Lisboa
Av. Rovisco Pais, 1
1049-001 Lisboa
Portugal
E-mail: patricia.figueiredo@tecnico.ulisboa.pt

Methods Inf Med 2015; 54: 232–239
http://dx.doi.org/10.3414/ME13-02-0052
received: November 5, 2013
accepted: December 16, 2014
epub ahead of print: April 24, 2015

1. Introduction

The concept of effective connectivity, describing the causal relation between activity in different brain areas, has been the subject of several works (and controversy) in the neuroimaging community over the last years [1]. A number of different approaches to modelling effective brain connectivity have been proposed, which differ in their choice of observation equation (how brain states translate into a measured signal) and evolution of the brain states with time. Notably, Dynamic Causal Modelling (DCM) is a biophysically inspired model-driven approach [2], which was introduced as a generic formalism for studying effective connectivity based on functional Magnetic Resonance Imaging (fMRI) and has since been the object of a number of extensions. Model inversion is achieved using Bayesian methods that approximate the evidence of each model by using a lower-bound to the model evidence, the free-energy. This is then typically combined with Bayesian model comparison, in order to allow the selection of the connectivity model that best explains the data among a set of plausible competing hypotheses.

In DCM, the average neuronal activity representing each brain area within a network is described by a bilinear dynamical system, which takes into account the intrinsic connectivity between brain areas as well as exogenous inputs both acting on regional activities and modulating connectivity strengths. A haemodynamic forward

model is used to describe the system output, that is the blood oxygenation level dependent (BOLD) signal measured using fMRI, as a function of the underlying neuronal activity. This is a single-input single-output (SISO) state-space model based on the balloon model proposed by Buxton et al. [3], and further analysed and complemented with the flow dynamics by Friston et al. [4]. It consists of four haemodynamic states (vasodilatory signal, blood flow, volume and deoxyhemoglobin content) that mediate between neuronal activity and the BOLD signal.

In the original DCM formulation, all the uncertainty is in the model parameters, while the time-course of the states is deterministic. This fails to take into account unmodelled (stochastic) dynamics, which are not caused by the known exogenous inputs or by the brain regions in the specified network. In order to address this, stochastic DCM (sDCM) was recently proposed [5]. The main departure from the deterministic DCM is the assumption of additive noise in the motion of the state variables, that is, the evolution of the states is given by stochastic differential equations. This introduces uncertainty in the state values and inputs, which can be estimated by the procedure used to invert the system (Dynamic expectation maximization (DEM) [6] or Generalised filtering (GF) [7]). Using sDCM will therefore also allow the estimation of unknown inputs, that is, spontaneous activity.

Different techniques for state estimation or model identification of stochastic dynamic systems have been developed. Under the assumptions of linearity and Gaussianity, Kalman Filter (KF) is optimal in the sense of maximum likelihood for state estimation [8]. When the model parameterisation is not completely known, a single KF may fail to obtain the correct state estimates [9]. An alternative consists of using several state observers in parallel, known as Multiple-Model Kalman Filtering (MMKF) [10]. In a MMKF approach, the relative probabilities of a number of pre-specified DCM models is computed. This feature makes this approach particularly suitable for addressing the problem of model selection in effective connectivity studies using DCM.

In this paper we present a MMKF algorithm for effective connectivity estimation based on stochastic DCM. We evaluate the performance of MMKF for selection between two plausible competing connectivity structures, and assess the impact of assuming state noise in the estimation.

2. Methods

In this Section, the integration of stochastic DCM equations is first presented, followed by the MMKF algorithm developed to perform model selection. Finally, we describe the Monte Carlo simulations performed in order to test the performance of the proposed algorithm.

2.1 Stochastic Dynamic Causal Modelling

The stochastic formulation of a bilinear DCM, for a brain network of n regions and m exogenous inputs, is described by the following differential equations. For the neuronal state:

$$dz = \left(\left(A + \sum_j u_j B^{(j)}\right) z + Cu\right) dt + C\sigma^{(v)} dW^{(v)} + \sigma^{(z)} dW^{(z)} \quad (1)$$

where $z_{n\times 1}(t)$ is the vector of neuronal activity in n regions; $u_{m\times 1}(t)$ is the vector of exogenous inputs; $A_{n\times n}$ is the intrinsic connectivity matrix, with negative diagonal terms (natural rate of decay of neuronal activity in each area) and non-zero off-diagonal terms representing connection strengths; each of the m matrices $B^{(j)}{}_{n\times n}$ is the connectivity modulation matrix, controlling the n × n modulation by input $u_j(t)$ on the connection strengths; $C_{n\times m}$ represents the direct influence of the exogenous inputs on the activity of each brain region; W(v) and W(z) are Wiener processes corresponding to the noise in the inputs and the state motion, respectively; and σ(v) and σ(z) are the corresponding standard deviations. In Equation 1, the time index t is dropped for simplicity.

Equation 1 is discretized through the integration in short time-steps, T, known as the Euler- Maruyama method (see Eq. 2 in Figure 1) where the σ values correspond to the log-precisions suggested in [5]. The difference of a Wiener process at two different time steps has a well-known normal distribution $(\aleph(0,T))$. The deterministic part of the system is linearized by assuming that the input is constant during a time-step, and can thus be readily integrated.

For the haemodynamic states and system output (see Eqs. 3–7 in Figure 2) where s is the vasodilatory signal (with 0 corresponding to steady-state); state variables f, v and q are the normalised blood flow, volume and deoxyhemoglobin content, respectively; ε is the neuronal efficacy; output y (i.e. the BOLD signal) is a nonlinear function of these state variables; k_s, k_f, τ, α and E_0 are the haemodynamic model parameters; V_0, k_1, k_2 and k_3 are BOLD signal parameters; $dW^{(h_s)}$, $dW^{(h_f)}$, $dW^{(h_v)}$ and $dW^{(h_q)}$ are the Wiener processes corresponding to the noise in the respective haemodynamic states; and $\sigma^{(h)}$ is the corresponding standard deviation. Equation 3 is linearized by a bilinear approximation [4], also assuming that inputs are constant in short time-intervals. The linearized equations are then discretized using the Euler-Maruyama method.

$$\begin{aligned} z(t+T) = \int_t^{t+T} & \left(\left(A + \sum_j u_j(t) B^{(j)}\right) z(\tau) + Cu(t)\right) d\tau \\ & + C\sigma^{(v)}\left(W^{(v)}(t+T) - W^{(v)}(t)\right) \\ & + \sigma^{(z)}\left(W^{(z)}(t+T) - W^{(v)}(t)\right) + z(t) \end{aligned} \quad (2)$$

Figure 1 Equation 2

$$ds = \left(\epsilon z - k_s s - k_f\left(f - 1\right)\right)dt + \sigma^{(h)} dW^{(h_q)} \quad (3)$$

$$df = s dt + \sigma^{(h)} dW^{(h_f)} \quad (4)$$

$$dv = \frac{1}{\tau}\left(f - v^{\frac{1}{\alpha}}\right)dt + \sigma^{(h)} dW^{(h_v)} \quad (5)$$

$$dq = \frac{1}{\tau}\left(f\frac{1-\left(1-E_0\right)^{\frac{1}{f}}}{E_0} - v^{\left(\frac{1}{\alpha}-1\right)}\right)dt + \sigma^{(h)} dW^{(h_q)} \quad (6)$$

$$y = V_0\left[k_1\left(1-q\right) + k_2\left(1-\frac{q}{v}\right) + k_3\left(1-v\right)\right] \quad (7)$$

Figure 2 Equations 3–7

2.2 Multiple-Model Kalman Filtering

The linearized and discretized sDCM neuronal and haemodynamic equations correspond to a linear state-space model with Gaussian white noise disturbances. A KF can then be used to estimate the noisy neuronal and haemodynamic states given a parameterized DCM. For the MMKF approach, a number of KFs are designed, each relevant to a different model with pre-assigned parameter values. The belief that each KF corresponds to the real system is updated recursively, according to:

$$P_i[k+1] \propto p\left(y[k+1]|\mathcal{H}_i, u[k], Y[k]\right) \cdot P_i[k] \quad (8)$$

where $P_i[k+1]$ is the probability of the i-th model $\mathcal{H}_i$, after observing the $(k+1)^{th}$ data point, and given the previous inputs u[k] and data points Y[k].

The fundamental assumption is that one of the models in the MMKF corresponds to the true model. In this case, the MMKF converges to the true model (i.e. the probability assigned tends to 1 as the amount of data tends to infinity). However, even if the true model is not in the set considered in the MMKF (which is almost certain to happen in a continuous parameter space), it will converge to the model that is closest to the real system in terms of the measure defined by Baram [11].

For each connectivity model structure belonging to the set of pre-specified plausible alternatives, the parameter space is discretized by sub-dividing each parameter interval into three equal parts. A subset of KFs is then generated for that connectivity structure corresponding to all the possible combinations of the discretized parameters. The probability of a given connectivity structure is finally given by the sum of the probabilities of all the KF that belong to the corresponding subset.

2.3 Simulations

For the simulations, we considered a previously reported scenario where two slightly different connectivity structures are compared [12] (▶ Figure 3). Each of them

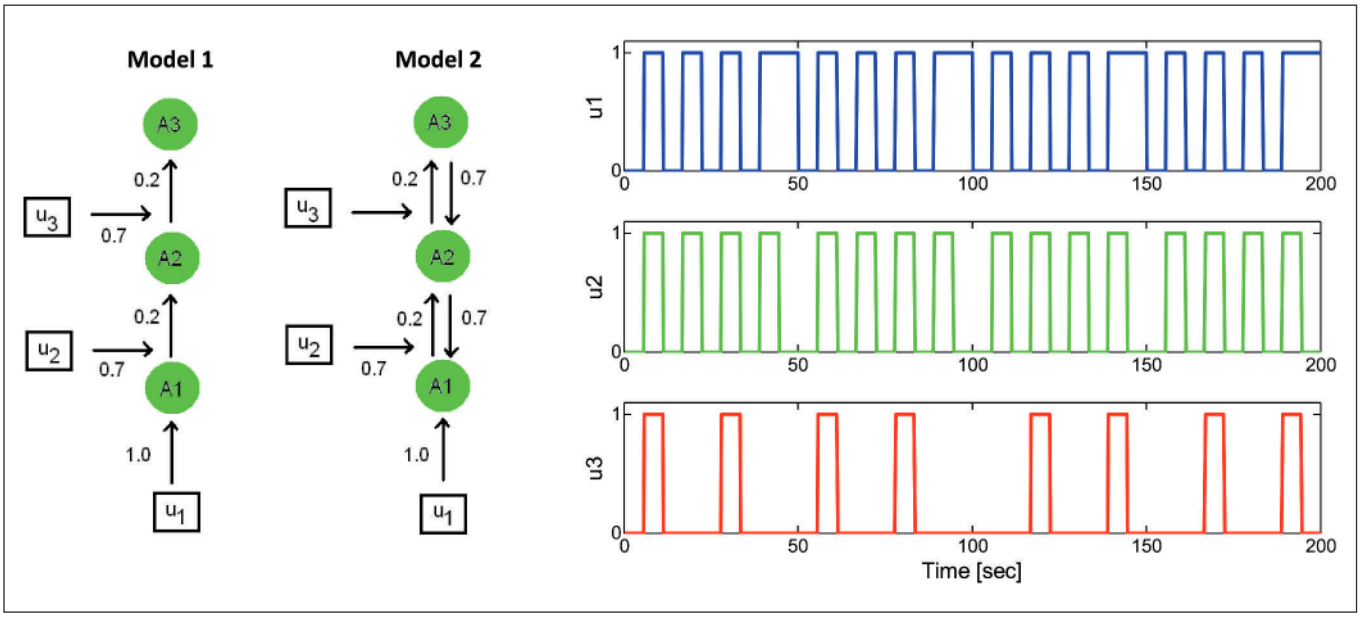

Figure 3 Connectivity models tested in the simulations: Model 1, with forward connections only, and Model 2, with both forward and reciprocal connections (left); and corresponding input time courses to the three brain regions (right). The feedforward and feedback connection weights are displayed in the figure by example, and correspond to the ones used in the example datasets used in Figure 4.

has three brain regions and represents one of two possible intrinsic connectivity structures, with and without reciprocal connections. The only difference between the models is hence that the second one exhibits backward connectivity, while the first one has only forward connectivity. The corresponding input time courses to the three brain regions are also shown in Figure 3.

For each of the two models, 25 simulations were performed. Each simulation consisted of 200 s of data generated with an integration step of 0.1 s and subsequent under-sampling to a repetition time, TR = 3 s. For each simulation, each of the neuronal model parameters was sampled from a uniform distribution in the interval (0.1, 0.9). Unless otherwise stated, the haemodynamic parameters were equal to the means of the priors in [2], as shown in Table 1, and the neuronal efficacy was ε = 1. The sensitivity of the model selection results to the variability of the haemodynamic parameters was evaluated by performing simulations with the respective values drawn from distributions around the mean priors with different standard deviations: σ = {0; 1; 10; 50; 100%}. Gaussian and white noise was added to the inputs, the states and the outputs, with variance such that the generated data have a specific signal-to-noise ratio (SNR). The following values were first tested: SNR = {0.1; 1.0; 100.0}, and a value of SNR = 5 was then used for further comparisons.

Table 1 Haemodynamic model parameter prior values

k_s	k_f			E_0
0.650 s^{-1}	0.410 s^{-1}	0.980 s	0.320	0.340

All hidden states (neuronal and haemodynamic) were recorded as well as the system output. Both MMKF assuming state noise equal to 0 (deterministic) and MMKF with correct variance (stochastic) were then run. Their hidden states estimates and the probabilities of each connectivity model were recorded. Two types of final model estimation were performed: using the estimates of the best KF (best), or the estimates of all KFs weighted by their probabilities (mixed).

In order to evaluate the accuracy of the estimated variables, the sum of squared errors, SSE, was computed for the neuronal and haemodynamic states as well as the system output:

$$SSE\left(s^{(l)},\ \hat{s}^{(l)}\right) = \sum_{k=1}^{N_t}\sum_{j=1}^{N_{regions}}\sum_{i=1}^{N_{time}}\left(s_{jk}^{(l)}(i) - \hat{s}_{jk}^{(l)}(i)\right)^2 \quad (9)$$

where i is the time-index, with N_{time} equal to the number of time points in the data, j is the region-index, with $N_{regions} = 3$, and $s^{(l)}$ is the k^{th} variable of region j of kind l, with $N_l = 1$ for the neuronal state and system output and $N_l = 4$ for the haemodynamic states.

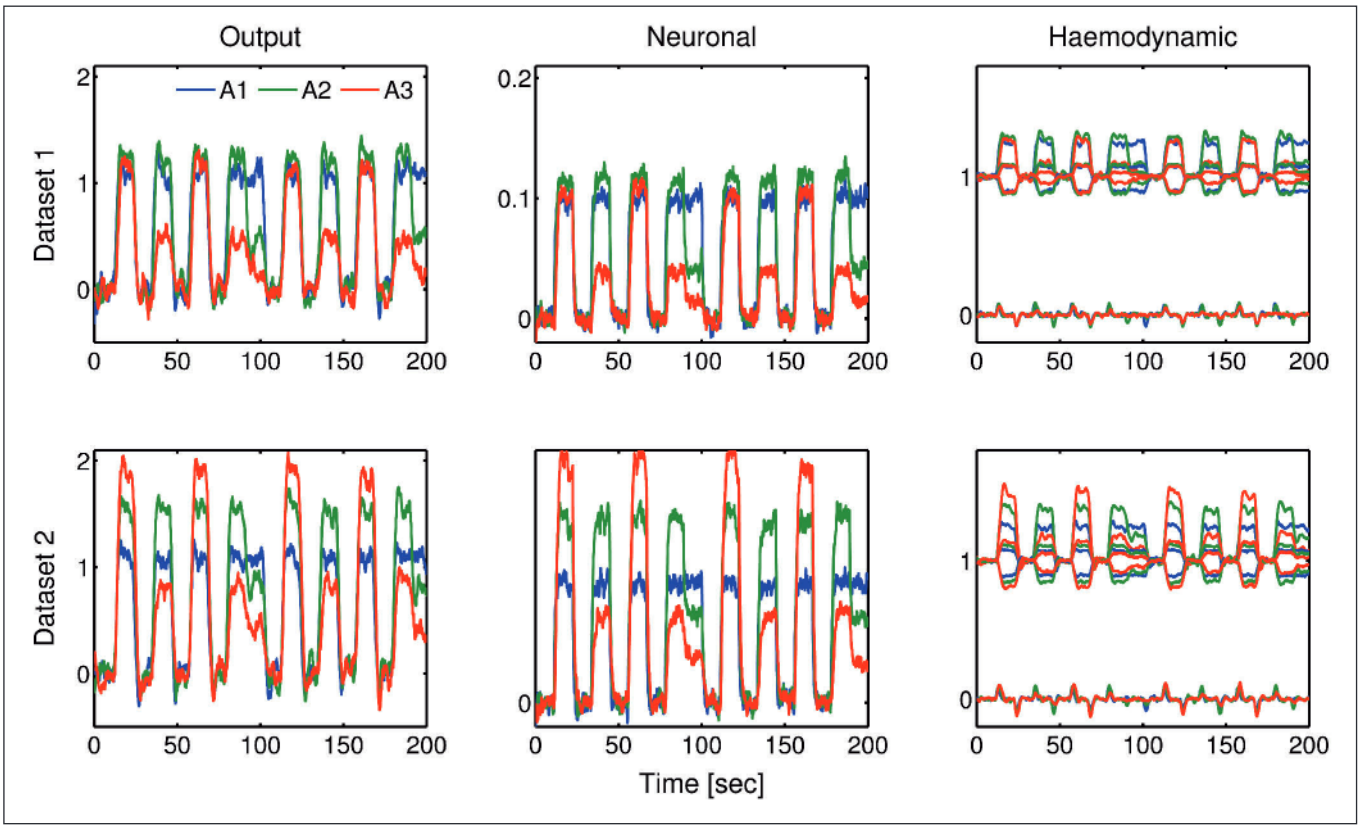

Figure 4 Time courses of the signal output, the neuronal state and the four haemodynamic states (vasodilatory signal (at 0, in phase with neuronal changes), blood flow and volume (at 1, in phase with neuronal changes) and deoxyhemoglobin), obtained in two example simulated datasets using Model 1 with different parameter settings, for the three brain regions (A1, A2 and A3).

This quantity was normalised by the mean of each estimated variable kind, in order to have an adimensional value comparable across variables (output, haemodynamic, neuronal). In order to evaluate the model selection accuracy, the final probability, P_i, of each of the two possible models was classified as strong evidence (S) if $0.95 \leq P_i$, positive evidence (P) if $0.75 \leq P_i < 0.95$, or weak evidence (W) if $0.50 \leq P_i < 0.75$.

3. Results

The time courses of the signal output, neuronal states and haemodynamic states, obtained in two example simulated datasets using Model 1 with different parameter settings, for the three brain regions (A1, A2 and A3), are shown in Figure 4. The model selection results obtained for different SNR values are shown in Figure 5. It can be observed that the SNR impacts the performance of the MMKF only for extremely low values (0.1), yielding reasonably similar results for SNR values between 1 and 10, which renders the chosen value SNR = 5 representative of the performance of the proposed algorithm. The model selection results obtained using different variances for the distribution of the haemodynamic parameters values are shown

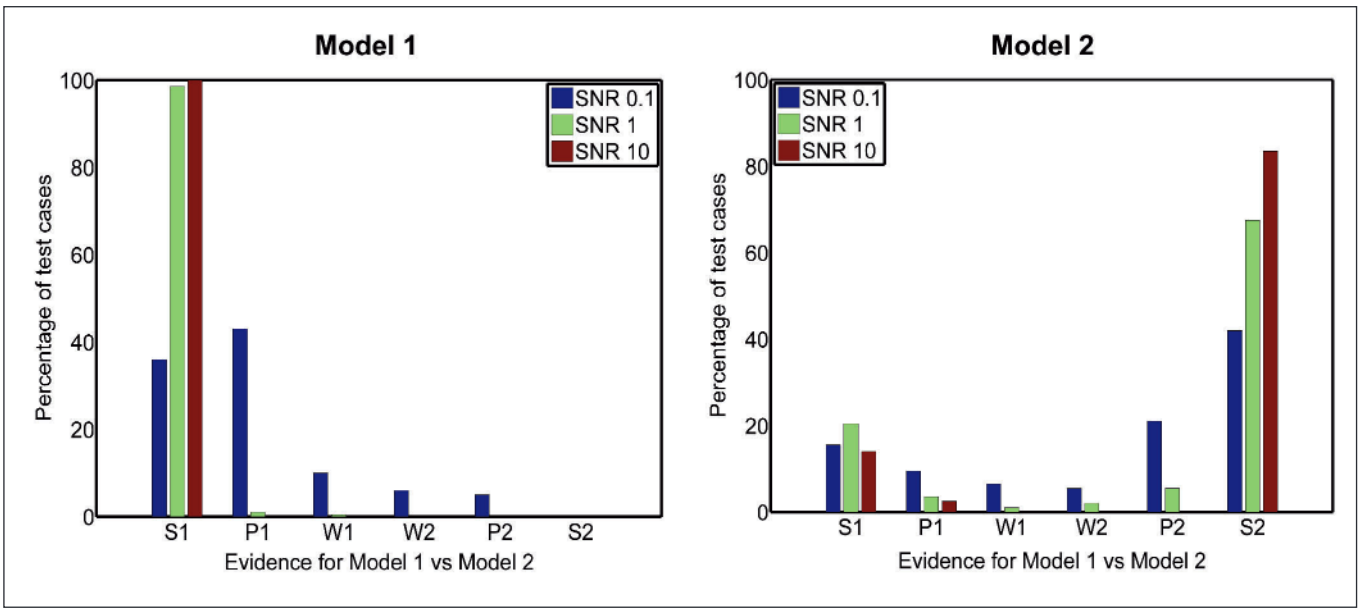

Figure 5 Distribution of the evidences (strong, S, positive, P, and weak, W) assigned to Model 1 (S1, P1, W1) and Model 2 (S2, P2, W2), by stochastic MMKF, using the mean HRF parameter values and different SNR values, for simulations of Model 1 (left) and Model 2 (right).

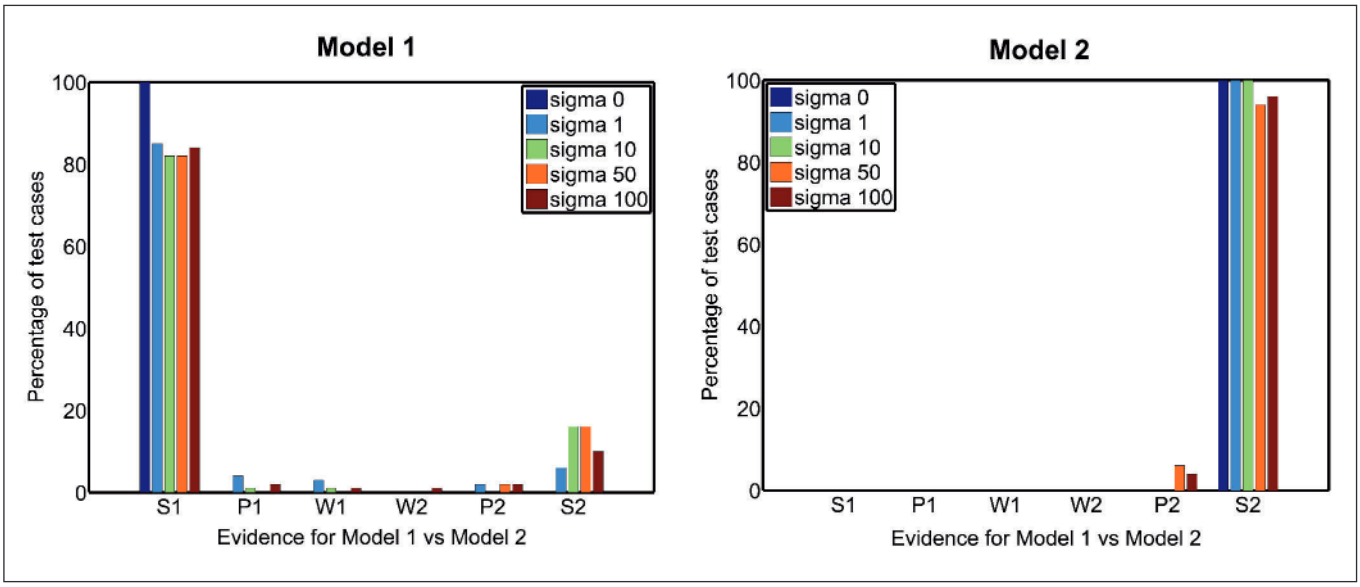

Figure 6 Distribution of the evidences (strong, S, positive, P, and weak, W) assigned to Model 1 (S1, P1, W1) and Model 2 (S2, P2, W2), by stochastic MMKF, using SNR = 5 and different HRF variance (sigma) values, for simulations of Model 1 (left) and Model 2 (right).

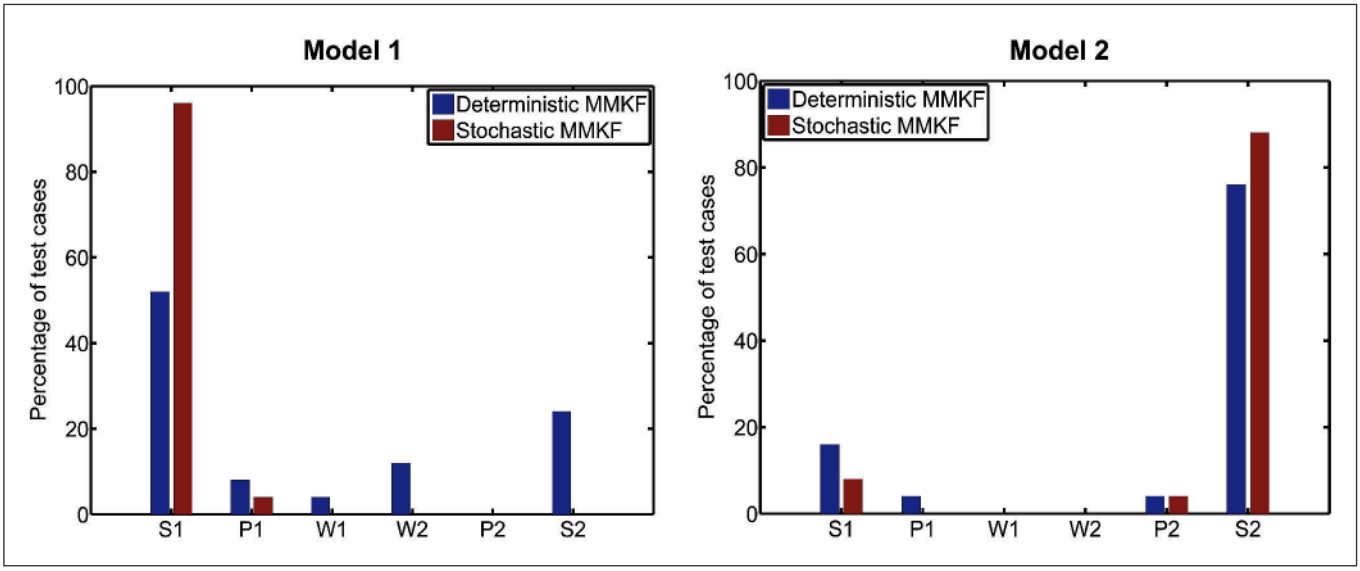

Figure 7 Distribution of the evidences (strong, S positive, P, and weak, W) assigned to Model 1 (S1, P1, W1) and Model 2 (S2, P2, W2), by deterministic and stochastic MMKF, for simulations of Model 1 (left) and Model 2 (right).

in Figure 6. It can be observed that haemodynamic variability has little impact on the performance of the MMKF, which renders the use their mean prior values a reasonable choice.

The model selection results obtained using both the deterministic and stochastic MMKF formulations are shown in Figure 7, for the simulations of Model 1 and Model 2. Regardless of which model is used to generate the data, deterministic MMKF has a greater tendency to choose the wrong structure than stochastic MMKF. Obviously, the deterministic model did not account for stochastic fluctuations of hidden states, and it also displayed a higher error rate due to a larger weighing of output values. In fact, the relatively high SNR makes the deterministic MMKF trust the output data more; since the MMKF does not contain any KF that represents the system exactly, the probabilities of each KF vary widely with time. In contrast, the stochastic MMKF introduces uncertainty in the transition between states, trusting the output data less and therefore yielding less variability in the probabilities. Since none of the KFs included in the MMKF algorithm correspond to the true model exactly, the probabilities of each KF in the deterministic approach may vary substantially with time. By accounting for state noise, stochastic MMKF has greater flexibility in tracking the hidden states, which allows for a few KFs to have significant probability assigned to them while most KFs are eliminated after a few seconds of data are processed.

The results for the state estimation obtained for Model 1 are shown in Figure 8 (similar results were obtained for Model 2, not shown). Although state estimation is not strictly performed by deterministic MMKF, the KF with highest probability should correspond to the one whose (deterministic) states are closest to the true ones, and these were therefore taken as the equivalent to the estimated states in this case. In stochastic MMKF, on the other hand, the states are treated as random variables with nonzero variance, thanks to the state noise, and estimated. As expected, the estimates by stochastic MMKF therefore outperform those by the deterministic MMKF. It is interesting to note that the best and mixed estimates have almost exactly the same error when using stochastic MMKF (i.e. the best KF already tracks the hidden states well), whereas deterministic MMKF benefits from a weighted estimate. Another interesting observation is that this improvement is more pronounced for the estimates of the haemodynamic states than for the neuronal states.

One possible application of the proposed methodology to real fMRI data is described here, as an example based on our own work [13]. In this study, we aimed to identify the seizure propagation pathway in a patient with epilepsy, by testing a set of clinically plausible effective brain connectivity models, based on fMRI data recorded during the occurrence of seizures. After standard pre-processing, the fMRI data were analysed using a general linear modelling approach in order to identify brain regions exhibiting seizure-related signal changes. A space of 16 connectivity models involving these regions was then defined according to the hypothesized seizure propagation pathways. A square waveform describing the periods of seizure activity was used as the system's input into the region known to be the epileptic focus in this case. A deterministic implementation of DCM was then employed in order to estimate the different connectivity models and Bayesian model comparison was subsequently applied to select the model with the highest evidence given the data. By using the stochastic MMKF methodology proposed here, we would be able to allow for perturbations in the system input, which would be more suitable to modelling spontaneous epileptic activity.

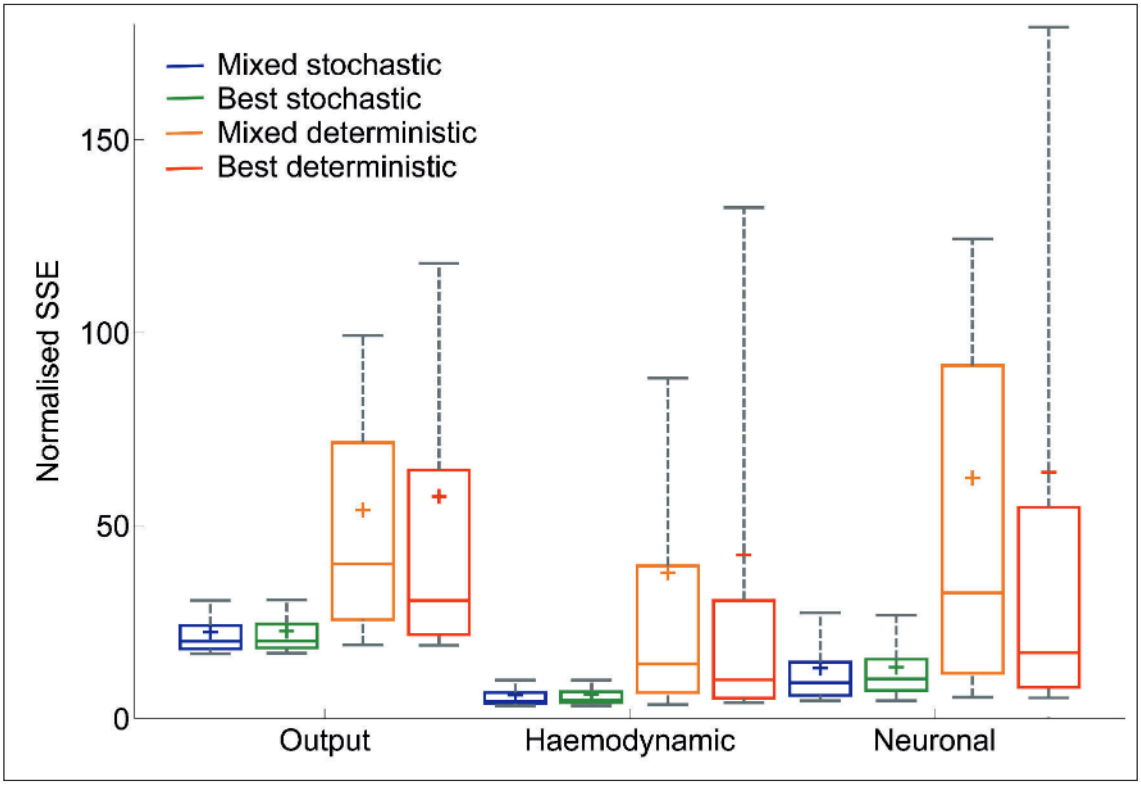

Figure 8
Distribution of normalised SSE values over the 25 simulations of Model 1, for output signal, haemodynamic states and neuronal states, using the best and mixed estimation methods, with both deterministic and stochastic MMKF. The box plots are delimited by the 25th and 75th percentiles, the whiskers extend over the 75% interval (between 12.5% and 87.5% percentiles), the median is indicated by the central dash and the mean is indicated by a cross.

4. Discussion and Conclusion

We have presented the first MMKF approach for the estimation of effective brain connectivity based on DCM. The proposed algorithm was able to successfully select the correct connectivity model structure from a set of pre-specified plausible alternatives. Moreover, we showed that MMKF assuming stochastic disturbances of the states was much more effective, not only in the selection of the correct connectivity model structure but also in the estimation of the hidden states, when com- pared with its deterministic counterpart. These results demonstrate the applicability of a MMKF approach to the study of effective brain connectivity using DCM of fMRI data, particularly when a stochastic formulation is desirable.

The growing interest in the study of resting-state functional connectivity (e.g. [14]) has in fact pressed for the development of appropriate methodologies for the study of connectivity in stochastic conditions, particularly using a DCM framework. Deterministic implementations of DCM presume that an extrinsic input is given to the brain network under investigation, corresponding to sensory stimulation or the performance of motor or cognitive tasks. However, accounting for stochastic fluctuations in neuronal activity and their interaction with task-specific processes may be of particular importance for studying state-dependent interactions. Also, allowing for random neuronal fluctuations may render DCM more robust to model misspecification and finesse problems with network identification [15]. Moreover, it is not possible to define such a deterministic input in studies of spontaneous brain activity, such as the one observed during resting-state or in pathological conditions like epilepsy.

In previous reports aiming to study effective connectivity within an epileptic network [13, 16–18], a deterministic implementation of DCM of fMRI was used and the system's input was conceived as a time marker of an initial event taking place within the postulated epileptic focus and which perturbs the associated network. Stochastic implementations of DCM will certainly provide more suitable approaches for modelling such epileptic spontaneous brain activities, since it accounts for endogenous or random fluctuations in hidden neuronal states. A recent paper has just demonstrated the first application of stochastic DCM to the study of the default mode network in first-episode schizophrenia [19]. Other applications of interest will target the study of resting-state networks measured by fMRI, under different brain states, physiological modulations or disease.

Despite their great potential, in the literature only a few methods have been proposed for model inversion (estimation) in the context of stochastic DCM. The original Bayesian estimation framework [2] was extended by the same authors to methods of dynamic expectation maximization, variational filtering and generalized filtering [5–7]. More recently, a nonlinear cubature Kalman filtering approach was proposed to invert models of coupled dynamical systems, which furnishes posterior estimates of both the hidden states and the parameters of the system, including any unknown exogenous input [20].

To the best of our knowledge, the methodology presented here is the first multiple-model approach to the problem of selecting the best brain effective connectivity structure among a set of hypotheses in the context of DCM. In a related context, we have previously developed a multiple-model framework for the identification of the haemodynamic response function (HRF) model from fMRI data [21]. In this case, Set-Valued Observers (SVOs) were used, whereby the HRF identification is put forward as a problem of model falsification or invalidation in which we are interested in distinguishing among a set of eligible models of dynamic systems.

It should be noted that the performance assessment of the proposed methodology is still preliminary. Firstly, it is limited to two connectivity structures, which have previously been used to test DCM for fMRI. Secondly, performance is assessed only on simulated data, and no challenge on real data is attempted. Finally, no comparison with other DCM identification methods was performed. In particular, a comparison with variational estimation followed by Bayesian model selection would be required in order to identify the strengths and weaknesses of the proposed algorithm relative to the current most common procedure.

Furthermore, the following points need to be addressed in the current form of the proposed algorithm. The SNR of the data should be estimated in order to make the algorithm robust to temporal scaling in the DCM matrices as well as to the amplitude of the signals. Moreover, a practical way of applying the algorithm without knowledge of the HRF for each area must also be developed. Finally, finding automatic techniques to design the optimal input for a given connectivity structure distinction would also have interesting applications. Future work should address these current limitations, in order to improve the proposed MMKF algorithm and completely characterize its performance and applicability in real fMRI data.

Acknowledgments

We acknowledge the Portuguese Science Foundation (FCT) for financial support through grants PTDC/SAU-ENB/112294/2009, PTDC/BBB-IMG/2137/2012 and FCT [UID/EEA/50009/2013].

References

1. Valdes-Sosa PA, Roebroeck A, Daunizeau J, Friston K. Effective connectivity: Influence, causality and biophysical modeling. NeuroImage 2011.
2. Friston KJ, Harrison L, Penny WD. Dynamic Causal Modelling. NeuroImage 2003; 19 (4): 1273–1302.
3. Buxton RB, Wong EC, Frank LR. Dynamics of blood flow and oxygenation changes during brain activation: the balloon model. Magn Reson Med 1998; 39 (6): 855–864. Available from: http://view.ncbi.nlm.nih.gov/pubmed/9621908.
4. Friston KJ, Mechelli A, Turner R, Price CJ. Nonlinear responses in fMRI: The Balloon model, Volterra kernels and other hemodynamics. NeuroImage 2000; 12: 466–477.
5. Li B, Daunizeau J, Stephan K, Penny W, Friston K. Stochastic DCM and generalized filtering. NeuroImage 2011.
6. Friston K, Trujillo-Barreto N, Daunizeau J. DEM: a variational treatment of dynamic systems. NeuroImage 2008; 41 (3): 849–885.
7. Friston K, Stephan K, Li B, Daunizeau J. Generalised filtering. Mathematical Problems in Engineering 2010; 2010 (Article ID 621670): 1–35.
8. Kalman RE. A New Approach to Linear Filtering and Prediction Problems. Transactions of the ASME–Journal of Basic Engineering 1960; 82 (Series D): 35–45.
9. Athans M, Falb PL. Optimal control: an introduction to the theory and its applications. New York: McGraw-Hill; 1966.
10. Murray-Smith R, Johansen TA, editors. Multiple Model Approaches to Modelling and Control. Taylor and Francis systems and control book series. London, UK: Taylor and Francis; 1997. Available from: http://eprints.gla.ac.uk/34147/.
11. Baram Y, Sandell N. An information theoretic approach to dynamical systems modeling and identification. IEEE Trans on Automatic Control 1978; 23 (1): 61–66.
12. Penny WD, Stephan KE, Mechelli PS, Friston KJ. Comparing Dynamic Causal Models. Neuroimage 2004; 22: 1157–1172.
13. Murta T, Leal A, Garrido MI, Figueiredo P. Dynamic Causal Modelling of epileptic seizure propagation pathways: A combined EEG/fMRI study. NeuroImage 2012; 62 (3): 1634–1642.
14. Griffanti L, Baglio F, Lagan MM, Pret MG, Cecconi P, Clerici M, et al. Individual Thresholding of Voxel-based Functional Connectivity Maps. Estimation of Random Errors by Means of Surrogate Time Series. Methods Inf Med 2014; 53 (4).
15. Daunizeau J, Stephan KE, Friston KJ. Stochastic dynamic causal modelling of fMRI data: Should we care about neural noise? NeuroImage 2012; 62 (1): 464–481.
16. Hamandi K, Powell HWR, Laufs H, Symms MR, Barker GJ, Parker GJM, et al. Combined EEG-fMRI and tractography to visualise propagation of epileptic activity. Journal of Neurology, Neurosurgery and Psychiatry 2008; 79 (5): 594–597.
17. David O, Guillemain I, Saillet S, Reyt S, Deransart C, Segebarth C, et al. Identifying neural drivers with functional MRI: an electrophysiological validation. PLoS Biol 2008; 6 (12): 2683–2697.
18. Vaudano A, Laufs H, Kiebel S, Carmichael D, Hamandi K, Guye M, et al. Causal hierarchy within the thalamo-cortical network in spike and wave discharges. PLoS One 2008; 4 (8): e6475.
19. Bastos-Leite AJ, Ridgway GR, Silveira C, Norton A, Reis S, Friston KJ. Dysconnectivity within the Default Mode in First-Episode Schizophrenia: A Stochastic Dynamic Causal Modeling Study with Functional Magnetic Resonance Imaging. Schizophrenia Bulletin 2014.
20. Havlicek M, Friston KJ, Jan J, Brazdil M, Calhoun VD. Dynamic modeling of neuronal responses in fMRI using cubature Kalman filtering. NeuroImage.
21. Silvestre C, Figueiredo P, Rosa P. Multiple-Model Set-Valued Observers: A new tool for HRF model selection in fMRI. Conf Proc IEEE Eng Med Biol Soc 2010; 1: 5704–5707. Available from: http://www.biomedsearch.com/nih/Multiple-Model-Set-Valued-Observers/21097322.html.